# Uncoupling protein 2 modulates polarization and metabolism of human primary macrophages via glycolysis and the NF-κB pathway

LIGUO LANG*, DONGJU ZHENG*, QINGJUN JIANG, TING MENG, XIAOHU MA and YANG YANG

Department of Cardiology, People's Hospital of Ningxia Hui Autonomous Region, Yinchuan, Ningxia Hui Autonomous Region 750001, P.R. China

Received May 21, 2023; Accepted August 17, 2023

DOI: 10.3892/etm.2023.12282

**Abstract.** Metabolic abnormalities, particularly the M1/M2 macrophage imbalance, play a critical role in the development of various diseases, leading to severe inflammatory responses. The present study aimed to investigate the role of uncoupling protein 2 (UCP2) in regulating macrophage polarization, glycolysis, metabolic reprogramming, reactive oxygen species (ROS) and inflammation. Primary human macrophages were first polarized into M1 and M2 subtypes, and these two subtypes were infected by lentivirus-mediated UCP2 overexpression or knockdown, followed by enzyme-linked immunosorbent assay, reverse transcription-quantitative PCR, western blotting and flow cytometry to analyze the effects of UCP2 on glycolysis, oxidative phosphorylation (OXPHOS), ROS production and cytokine secretion, respectively. The results demonstrated that UCP2 expression was suppressed in M1 macrophages and increased in M2 macrophages, suggesting its regulatory role in macrophage polarization. UCP2 overexpression decreased macrophage glycolysis, increased OXPHOS, decreased ROS production, and led to the conversion of M1 polarization to M2 polarization. This process involved NF-κB signaling to regulate the secretion profile of cytokines and chemokines and affected the expression of key enzymes of glycolysis and a key factor for maintaining mitochondrial homeostasis (nuclear respiratory factor 1). UCP2 knockdown in M2 macrophages exacerbated inflammation and oxidative stress by promoting glycolysis, which was attenuated by the glycolysis inhibitor 2-deoxyglucose. These findings highlight the critical role of UCP2 in regulating macrophage polarization, metabolism, inflammation and oxidative stress through its effects on glycolysis, providing valuable insights into potential therapeutic strategies for macrophage-driven inflammatory and metabolic diseases.

*Correspondence to:* Dr Liguo Lang, Department of Cardiology, People's Hospital of Ningxia Hui Autonomous Region, 301 Zhengyuan North Street, Jinfeng, Yinchuan, Ningxia Hui Autonomous Region 750001, P.R. China
E-mail: langliguo1633@outlook.com

*Contributed equally

*Abbreviations:* LPS, lipopolysaccharide; IFN-γ, interferon γ; M0, non-polarized macrophages; UCP2, uncoupling protein 2; TNF-α, tumor necrosis factor α; IL, interleukin; RT-qPCR, reverse transcription-quantitative PCR; ROS, reactive oxygen species; HK2, hexokinase 2; PFK, phosphofructokinase; LDHA, lactate dehydrogenase A; PGC-1α, peroxisome proliferator-activated receptor γ coactivator 1-α; NRF1, nuclear respiratory factor 1; 2-DG, 2-deoxyglucose; ELISA, enzyme-linked immunosorbent assay; CXCL, C-X-C motif chemokine ligand; CCL, C-C motif chemokine ligand; OXPHOS, oxidative phosphorylation

*Key words:* UCP2, glycolysis, OXPHOS, macrophage polarization, NF-κB

## Introduction

Metabolic abnormalities, particularly imbalances in macrophage polarization, are critical factors in the pathogenesis of several diseases, including inflammation, autoimmunity and metabolic disorders (1,2). Under various stimuli, macrophages display remarkable plasticity, switching between pro-inflammatory M1 and anti-inflammatory M2 phenotypes (3,4). When lipopolysaccharide (LPS) and interferon (IFN) activate M1 macrophages, they release pro-inflammatory cytokines such tumor necrosis factor (TNF), interleukin (IL)-1 and IL-6 that cause tissue damage and inflammation (5). On the other hand, M2 macrophages can be induced by IL-4 cytokines and secrete anti-inflammatory factors such as IL-10 and TGF-β, promoting tissue repair and resolution of inflammation (6). However, imbalances in M1/M2 macrophage transitions can lead to severe inflammatory responses and oxidative stress, posing significant obstacles to disease treatment and prognosis (7). This process involves interactions between macrophage polarization, metabolic reprogramming, reactive oxygen species (ROS) and inflammation (8,9). Therefore, the study of macrophage polarization is essential for understanding the pathological mechanisms of metabolic diseases.

Metabolic reprogramming is a core process of macrophage polarization, with M1 macrophages relying on glycolysis for rapid energy production and M2 macrophages

using oxidative phosphorylation (OXPHOS) for more sustained energy supply (10). Uncoupling protein 2 (UCP2) is a member of the mitochondrial anion carrier protein family located in the inner mitochondrial membrane that can reduce ROS production by dissipating the proton gradient, thereby affecting cellular metabolism and energy balance (11,12). Previous studies have suggested that UCP2 may play a critical role in regulating macrophage phenotypic transitions and may be involved in coordinating macrophage glycolysis, OXPHOS and ROS generation (13-15). However, the exact mechanisms by which UCP2 regulates macrophage polarization, glycolysis and inflammation remain unclear.

The NF-κB signaling pathway is an important regulator of immune and inflammatory responses, cell survival and proliferation (16,17). Its activation can increase the expression of glycolytic enzymes such as hexokinase 2 (HK2), phosphofructokinase (PFK) and lactate dehydrogenase A (LDHA), thereby promoting glycolysis (18,19). In addition, research has shown that NF-κB signaling mediated inflammatory responses can inhibit peroxisome proliferator-activated receptor γ coactivator 1-α (PGC-1α), potentially leading to reduced activity of nuclear respiratory factor 1 (NRF1), a critical factor in maintaining mitochondrial homeostasis, which in turn may result in decreased mitochondrial biogenesis and impaired oxidative metabolism (20,21).

The present study aimed to elucidate the role of UCP2 in modulating macrophage polarization by examining its effects on M1/M2 homeostasis, glycolysis, mitochondrial function, cytokine and chemokine secretion and glycolytic enzyme expression. These findings may provide new insights into the molecular mechanisms underlying UCP2-mediated macrophage polarization and explore the potential therapeutic implications of targeting UCP2 in inflammatory and immune-mediated diseases.

## Materials and methods

*Cell culture and macrophage differentiation*. Peripheral blood mononuclear cells from six healthy volunteers from the People's Hospital of Ningxia Hui Autonomous Region (approval number 2022319) were isolated by density gradient centrifugation and $CD14^+$ magnetic bead isolation (Thermo Fisher Scientific, Inc.) following the guidelines of the Declaration of Helsinki. Isolated monocytes were cultured in RPMI 1640 medium (Gibco; Thermo Fisher Scientific, Inc.), supplemented with 10% fetal bovine serum (Gibco; Thermo Fisher Scientific, Inc.) and 50 ng/ml macrophage colony-stimulating factor (Invitrogen; Thermo Fisher Scientific, Inc.). The cells were incubated at 37˚C in a humidified atmosphere with 5% $CO_2$ for seven days to induce differentiation into M0 macrophages.

*Macrophage polarization*. Post differentiation, for M1 macrophage polarization, M0 macrophages were treated with a combination of 100 ng/ml LPS (MilliporeSigma) and 20 ng/ml IFN-γ (MilliporeSigma) for 48 h at 37˚C. The M0 macrophages were also treated with 20 ng/ml IL-4 (MilliporeSigma) for 48 h at 37˚C to achieve M2 polarization. The treatment medium was replaced every 24 h to maintain effective concentrations of the cytokines. After polarization, cells were analyzed by flow cytometry to confirm successful polarization, as described below.

*Lentivirus production and infection*. Lentivirus for UCP2 overexpression and knockdown was produced using a 3rd generation lentiviral generation system in 293T cells. For transfection, 10 μg lentiviral plasmid was used in combination with the lentiviral packaging plasmid psPAX2 and the envelope plasmid pMD2.G at a ratio of 4:3:3, respectively. The cells were co-transfected with the appropriate vector, either the UCP2 cDNA cloned into a pLVX-IRES-ZsGreen1 vector for overexpression (ov-UCP2) (Shanghai GenePharma Co., Ltd.) or short hairpin RNA (shRNA) for UCP2 knockdown (cat. no. EHU007971; MilliporeSigma), the sequence of which is: Sense, 5'-GAGACAUUGGCCUGAAAUCGUCUUCAAGAGAGACGAUUUCAGGCCAAUGUCU-3' and antisense, 5'-GCUAAAGUCCGGUUACAGAUCUCUCUUGAAGAUCUGUAACCGGACUUUAGC-3', integrated into a PLKO.1 vector. As a negative control for both overexpression (ov-NC) and knockdown (sh-NC) of UCP2, cells were co-transfected with an empty pLVX-IRES-ZsGreen1 or PLKO.1 vector. Transfections were performed using Lipofectamine 3000 (Invitrogen; Thermo Fisher Scientific, Inc.), according to the manufacturer's instructions, along with the lentivirus packaging plasmids pMD2.G and psPAX2. Lentivirus-containing supernatants were harvested 48 to 72 h after transfection and centrifuged at 100,000 x *g* for 2 h at 4˚C. Lentiviral particles were resuspended with PBS and added to the medium at a multiplicity of infection of 50, supplemented with 4 μg/ml of polybrene (Beyotime Institute of Biotechnology) to enhance the efficiency of infection. After a subsequent incubation of 48 h, cells were subjected to puromycin (Beyotime Institute of Biotechnology) selection at a concentration of 2 μg/ml for 48 h. A lower concentration (1 μg/ml) of puromycin was used for maintenance. The cells were then incubated for a further 72 h under normal conditions before being used for subsequent experimental analyses.

*Flow cytometry assay*. Using flow cytometry, ROS levels and macrophage surface markers were examined. CD68-phycoerythrin (PE) (dilution, 1:500; cat. no. 12-0689-41), CD86-allophycocyanin (dilution, 1:500; cat. no. 17-0869-42) and CD206-PE (dilution, 1:500; cat. no. 12-2069-42) antibodies (Invitrogen; Thermo Fisher Scientific, Inc.) were used to label the cells, which were then examined using a BD FACSCanto II flow cytometer (BD Biosciences). Cells were exposed to the fluorescent probe 2',7'-dichlorodihydrofluorescein diacetate (MilliporeSigma) before being examined by flow cytometry (BD FACSDiva software v9.0; BD Biosciences) to detect ROS. The flow cytometry assay was repeated three times.

*Enzyme-linked immunosorbent assay (ELISA)*. Culture supernatants were collected, and the levels of TNF-α (cat. no. SEKH-0047), IL-1β (cat. no. SEKH-0002), IL-6 (cat. no. SEKH-0013), IL-10 (cat. no. SEKH-0018), TGF-β (cat. no. SEKH-0316), C-X-C motif chemokine ligand (CXCL)2 (cat. no. SEKH-0066), CXCL9 (cat. no. SEKH-0245), CXCL10 (cat. no. SEKH-0070), C-C motif chemokine ligand (CCL)17 (cat. no. SEKH-0315), CCL22 (cat. no. SEKH-0239) and CCL24 (cat. no. SEKH-0063) were quantified using commercial ELISA kits (Beijing Solarbio Science & Technology Co.,

Ltd.) according to the manufacturer's instructions. ELISA assay was repeated three times.

*Assay of cellular ATP levels*. An ATP detection kit (cat. no. BC0305; Beijing Solarbio Science & Technology Co., Ltd.) was used according to the manufacturer's instructions. Sample preparation included the use of lysis buffer (Beyotime Institute of Biotechnology) for cell and tissue samples to ensure proper cell lysis at 4˚C. After centrifugation at 800 x g for 10 min at 4˚C, the supernatants were collected and mixed with the ATP detection working solution prepared. The chemiluminescence generated by the reaction was measured using an enzyme-labeled instrument (Thermo Fisher Scientific, Inc.) to determine the concentration of ATP in the samples. The assay was repeated three times.

*Reverse transcription quantitative PCR (RT-qPCR)*. TRIzol® reagent (Invitrogen; Thermo Fisher Scientific, Inc.) was used to extract total RNA from macrophages according to the manufacturer's instructions. A NanoDrop 2000 spectrophotometer (Thermo Fisher Scientific, Inc.) was used to measure the RNA concentration and purity for 5 sec at 21˚C. For cDNA synthesis, the SuperScript IV First-Strand Synthesis System (Invitrogen; Thermo Fisher Scientific, Inc.) was used according to the manufacturer's protocol. This comprises SuperScript IV reverse transcriptase, the accompanying 5X SSIV Buffer, 10 mM dNTP mix, and both oligo(dT)20 and random hexamer primers. The Applied Biosystems®7500 Real-Time PCR equipment (Thermo Fisher Scientific, Inc.) was utilized for the RT-qPCR analysis using the SYBR® Premix Ex Taq™ II kit (Takara Bio, Inc.). The PCR conditions were as follows: 95˚C for 32 sec, followed by 40 cycles of 95˚C for 6 sec and 62˚C for 32 sec. The $2^{-\Delta\Delta Cq}$ method (22) was used to calculate the levels of UCP2, HK2, PFK, LDHA, PGC-1 and NRF1 expression after normalizing them to the housekeeping gene GAPDH. The sequences of each primer utilized in this investigation were created by Shanghai GenePharma Co., Ltd., and they are all presented in Table I. RT-qPCR assay was repeated three times.

*Western blotting*. Cells were lysed with lysis buffer (Beyotime Institute of Biotechnology), and protein concentrations in the extracts were determined using a bicinchoninic acid protein assay kit (Beyotime Institute of Biotechnology) according to the manufacturer's instructions. Equal quantities of protein (20 $\mu$g/lane) were separated by SDS-PAGE (10%) and transferred onto nitrocellulose membranes (Cytiva) after macrophages were lysed using RIPA buffer (Beyotime Institute of Biotechnology). The membranes were treated with primary antibodies for an overnight period at 4˚C after being blocked with 5% BSA in Tris-buffered saline containing 0.1% Tween-20 for 1 h at 21˚C. The primary antibodies utilized in this investigation were all from Abcam and were anti-UCP2 (dilution, 1:1,000; cat. no. ab97931), anti-p65 (dilution, 1:1,000; cat. no. ab16502), anti-phospho-p65 (dilution, 1:2,000; cat. no. ab86299), and anti-GAPDH (dilution, 1:2,000; cat. no. ab181602). Membranes were cleaned with 10% tris-buffered saline-0.1% Tween-20 (v/v; Beijing Solarbio Science & Technology Co., Ltd.) before being incubated for 1 h at 21˚C with the Goat Anti-Rabbit IgG (HRP) secondary antibody (1:5,000; cat. no. ab205718; Abcam). SuperSignal West Pico PLUS Chemiluminescent Substrate (Thermo Fisher Scientific, Inc.) was used to see protein bands, and a ChemiDoc XRS+ Imaging System (Bio-Rad Laboratories, Inc.) was used to capture images of bands. ImageJ (version 1.48; National Institutes of Health) densitometric analysis was performed to analyze the bands. Western blotting was repeated three times.

Table I. Primer sequences for reverse transcription-quantitative PCR.

| Primers | Sequences (5'-3') |
|---|---|
| HK2 F | GCTTGCCTACTTCTTCACG |
| HK2 R | TTTCTCCATCTCCTTGCG |
| PFK F | ACAGAAGCCTTGGTCTAACAC |
| PFK R | GGAGAGTTGGAGGAATCAGTAG |
| LDHA F | TTCAGCCCGATTCCGTTAC |
| LDHA R | AGACACCAGCAACATTCATTCC |
| PGC-1α F | CACCAGCCAACACTCAGCTA |
| PGC-1α R | GTGTGAGGAGGGTCATCGTT |
| NRF1 F | AAACGGCCTCATGTATTTGAGT |
| NRF1 R | TAACGTGGCTCGAAGTTTCCG |
| UCP2 F | TCTGATGCCCAGAGAAGGGA |
| UCP2 R | AACTCTGCCGGAATAGGCAC |
| GAPDH F | GCTCATTTGCAGGGGGGAG |
| GAPDH R | GTTGGTGGTGCAGGAGGCA |

UCP2, uncoupling protein 2; HK2, hexokinase 2; PFK, phosphofructokinase; LDHA, lactate dehydrogenase A; PGC-1α, peroxisome proliferator-activated receptor γ coactivator 1-α; NRF1, nuclear respiratory factor 1; F, forward; R, reverse.

*Metabolic assays*. The extracellular acidification rate and $O_2$ consumption rate was assessed using a Seahorse XF96 Extracellular Flux Analyzer (Agilent Technologies, Inc.) in accordance with the manufacturer's instructions to examine glycolysis and oxidative phosphorylation in macrophages. Sequential injections of glucose, oligomycin and 2-deoxyglucose (2-DG) were used to evaluate the function of the glycolytic system of the cells, while sequential injections of oligomycin, carbonyl cyanide-4-(trifluoromethoxy)phenylhydrazone, and a combination of antimycin A and rotenone were used to assess the function of the mitochondrial system. The metabolic assay was repeated three times.

*Statistical analysis*. Data from at least three separate experiments are presented as mean ± standard deviation. One-way ANOVA analysis of variance was used for statistical comparisons, and Tukey's multiple comparison post hoc test was performed after that. $P<0.05$ was considered to indicate a statistically significant difference. GraphPad Prism 9.0 software (GraphPad Software, Inc.; Dotmatics) was used for all statistical analyses.

## Results

*M1 polarization suppresses UCP2 expression*. To confirm the successful polarization of primary human M0 macrophages

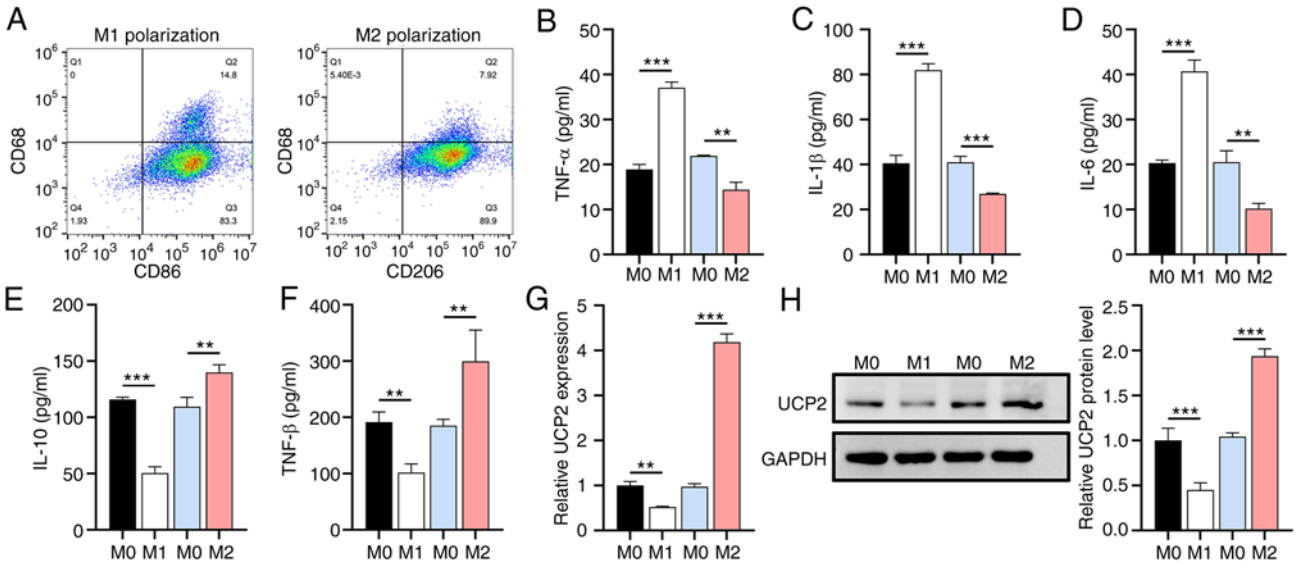


Figure 1. M1 polarization suppresses UCP2 expression in primary human macrophages. (A) Flow cytometry analysis of M1 ($CD68^+CD86^+$) and M2 ($CD68^+CD206^+$) macrophage populations following LPS and IFN-γ or IL-4 induction (n=6). ELISA results showing changes in pro-inflammatory (B) TNF-α, (C) IL-1β (D) and IL-6 and anti-inflammatory (E) IL-10 and (F) TGF-β cytokine secretion with different inductions (n=3). (G) RT-qPCR analysis of UCP2 mRNA expression levels in M1 and M2 macrophages (n=3). (H) Western blotting of UCP2 protein levels in M1 and M2 macrophages (n=3). $^{**}$P<0.01 and $^{***}$P<0.001. LPS, lipopolysaccharide; IFN-γ, interferon γ; IL, interleukin; TNF-α, tumor necrosis factor alpha; RT-qPCR, reverse transcription quantitative PCR; UCP2, uncoupling protein 2.

into M1 and M2 macrophages, subtype-specific surface markers and cytokines were analyzed. The flow cytometry results showed that LPS and IFN-γ induction increased the M1 macrophage population ($CD68^+CD86^+$), whereas IL-4 induction increased the M2 macrophage population ($CD68^+CD206^+$) (Fig. 1A). The ELISA results demonstrated that, under the impetus of LPS and IFN-γ, M0 macrophages facilitated an elevation in proinflammatory cytokines TNF-α, IL-1β, and IL-6 secretion by 96.12, 102.39 and 100.49% respectively, whilst experiencing a reduction of 34.25, 34.20 and 50.32% correspondingly under the influence of IL-4 (Fig. 1B-D). Contrariwise, the anti-inflammatory cytokines IL-10 and TGF-β diminished by 56.49 and 46.73%, respectively, under the stimulus of LPS and IFN-γ, yet they exhibited an increment of 27.90 and 61.70%, respectively, under the inducement of IL-4 (Fig. 1E and F). Subsequent analysis of M1 or M2 macrophage polarization on endogenous expression levels of UCP2 using RT-qPCR and western blotting revealed a significant increase in UCP2 expression in M2 macrophages and a decrease in M1 macrophages (Fig. 1G and H), suggesting a regulatory role for UCP2 in macrophage polarization.

*UCP2 overexpression decreases glycolysis and ATP synthesis and promotes OXPHOS and ROS*. To elucidate the metabolic effects of UCP2 on macrophages, all macrophage subtypes were infected with lentivirus expressing UCP2 to generate primary human macrophages overexpressing UCP2. Flow cytometry results indicated that, compared with the M0 ov-NC groups, there was an increase in the proportion of $CD86^+$ cells in the M1 ov-NC group, while the proportion of $CD206^+$ cells was decreased. By contrast, the M2 ov-NC group exhibited the opposite trend compared with the M1 ov-NC group. Furthermore, following UCP2 overexpression, compared with the M0, M1 and M2 ov-NC groups, the proportions of $CD86^+$ cells in the M0, M1 and M2 groups, respectively, were significantly reduced, while the proportions of $CD206^+$ cells were increased. This suggested that UCP2 increased the proportion of M2 macrophages ($CD206^+$ cells) and decreased the proportion of M1 macrophages ($CD86^+$ cells), regardless of their original subtype (Fig. 2A). M1 macrophages exhibited increased ROS levels and glycolytic rates and decreased OXPHOS levels compared with M0, whereas M2 macrophages showed the opposite trend (Fig. 2B-D). Furthermore, UCP2 overexpression significantly reduced glycolytic rates and increased OXPHOS levels in all macrophage subtypes, accompanied by a decrease in ATP synthesis (Fig. 2E), expression of key glycolytic enzymes such as HK2, PFK and LDHA (Fig. 2F-H), and an increase in expression of mitochondrial biogenesis markers PGC-1α and NRF1 (Fig. 2I and J).

*UCP2 overexpression regulates macrophage cytokine and chemokine secretion profiles through inhibition of NF-κB signaling*. Given the impact of UCP2 on macrophage polarization, the effect of UCP2 regulation on cytokine and chemokine secretion was further investigated. UCP2 overexpression in all macrophage subtypes resulted in a significant decrease in pro-inflammatory chemokines (CXCL2, CXCL9 and CXCL10) and cytokines (TNF-α, IL-1β and IL-6) (Fig. 3A-F) compared with the M2 ov-NC group, whereas anti-inflammatory chemokines (CCL17, CCL22, and CCL24) and cytokines (IL-10 and TGF-β) were significantly increased (Fig. 3G-K). The RT-qPCR results revealed an elevation in UCP2 expression by 279.45% within the ov-UCP2 group of M0 macrophages when compared against the ov-NC group. Additionally, M1 polarization contributed to a 48.94% decrease in UCP2 expression compared with the M0 ov-NC group, while M2 polarization stimulated an increase of 305.85%. Within M1 macrophages, UCP2 expression in the UCP2 group saw an

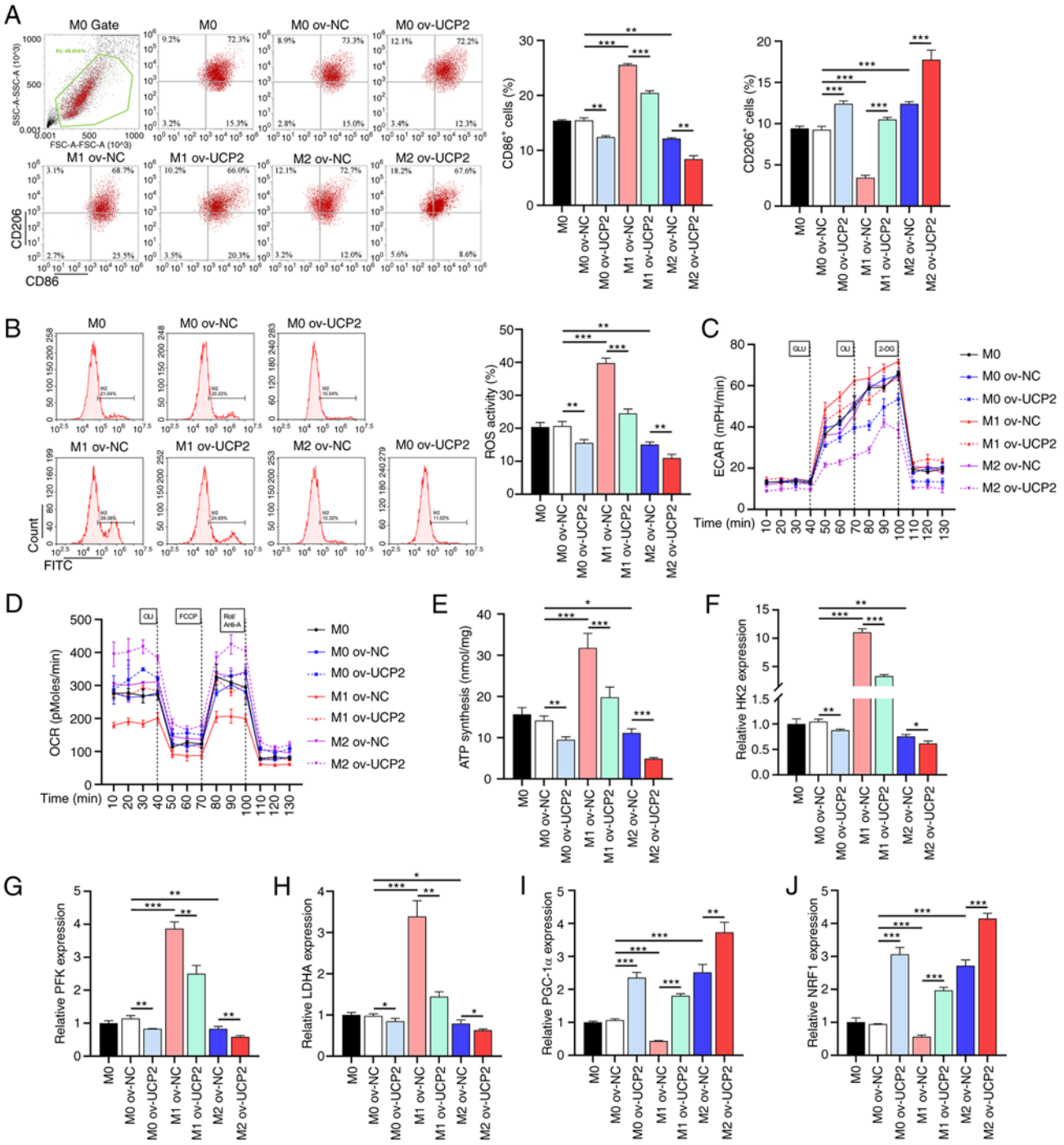


Figure 2. UCP2 overexpression alters macrophage metabolism and polarization. (A) Flow cytometry analysis of M1-to-M2 macrophage conversion with UCP2 overexpression (n=3). (B) ROS levels, (C) ECAR and (D) OCR in macrophages with UCP2 overexpression (n=3). (E) ATP synthesis in macrophages with UCP2 overexpression (n=3). RT-qPCR analysis of key glycolytic enzymes (F) HK2, (G) PFK and (H) LDHA in UCP2-overexpressing macrophages (n=3). RT-qPCR analysis of mitochondrial biogenesis markers (I) PGC-1α and (J) NRF1 in UCP2-overexpressing macrophages (n=3). $^{*}$P<0.05, $^{**}$P<0.01, $^{***}$P<0.001. RT-qPCR, reverse transcription quantitative PCR; ROS, reactive oxygen species; OXPHOS, oxidative phosphorylation; UCP2, uncoupling protein 2; HK2, hexokinase 2; PFK, phosphofructokinase; LDHA, lactate dehydrogenase A; PGC-1α, peroxisome proliferator-activated receptor g coactivator 1-α; NRF1, nuclear respiratory factor 1; ov-, overexpression; NC, negative control; ECAR, extracellular acidification rate; OCR, $O_2$ consumption rate.

increase of 323.21% as compared with the ov-NC group. In M2 macrophages, the UCP2 group reported an increase of UCP2 expression by 53.76% when compared with the ov-NC group (Fig. 3L). Western blotting illuminated notable fluctuations in protein levels within M0 macrophages, relative to the ov-NC group. Specifically, UCP2 overexpression resulted in a 47.72% increase in UCP2 protein levels and a 14.40% decrease in the p-p65/p65 ratio, respectively, compared with the M0 ov-NC group. Furthermore, M1 polarization instigated a 43.36% reduction and a 36.53% increase in UCP2 expression and the p-p65/p65 ratio, respectively. Conversely, M2 polarization induced a 27.81% increase in UCP2 expression and a decrease of 17.44% in the p-p65/p65 ratio. Within the ambit of M1 macrophages, the UCP2 group exhibited a 92.21% increase in

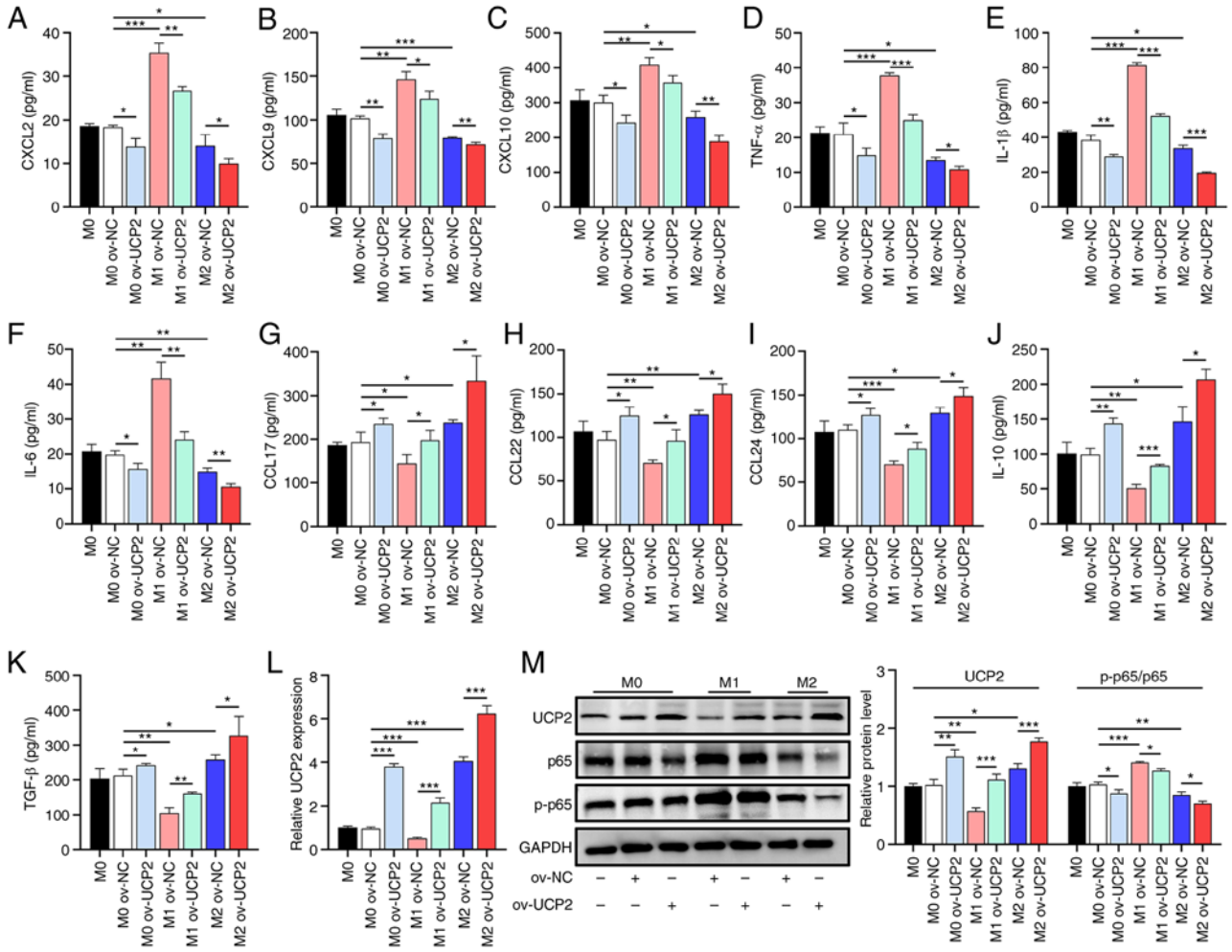


Figure 3. UCP2 overexpression modulates macrophage cytokine and chemokine secretion through NF-κB signaling inhibition. ELISA results showing changes in pro-inflammatory (A) CXCL2, (B) CXCL9, (C) CXCL10, (D) TNF-α, (E) IL-1β (F) and IL-6 and anti-inflammatory (G) CCL17, (H) CCL22, (I) CCL24, (J) IL-10 and (K) TGF-β chemokine and cytokine secretion with UCP2 overexpression (n=3). (L) RT-qPCR analysis of UCP2 mRNA expression in macrophages with UCP2 overexpression (n=3). (M) Western blotting of UCP2 protein levels and the ratio of p-p65/p65 in macrophages with UCP2 overexpression (n=3). $^{*}$P<0.05, $^{**}$P<0.01, $^{***}$P<0.001. RT-qPCR, reverse transcription quantitative polymerase chain reaction; CXCL, C-X-C motif chemokine ligand; CCL, C-C motif chemokine ligand; p65, NF-κB p65 subunit; UCP2, uncoupling protein 2; ov-, overexpression; NC, negative control; p-, phosphorylated.

UCP2 protein levels and a drop of 10.07% in the p-p65/p65 ratio compared with the ov-NC group. Similarly, within M2 macrophages, the UCP2 group exhibited a 36.27% increase in UCP2 and a reduction of 16.64% in the p-p65/p65 ratio compared with the ov-NC group (Fig. 3M).

*UCP2 knockdown exacerbates inflammation and oxidative stress by promoting macrophage glycolysis through lentivirus-mediated approach*. To further confirm the role of UCP2 in macrophage inflammation and oxidative stress, a lentivirus-mediated UCP2 knockdown experiment in M2 macrophages was performed. The RT-qPCR results confirmed that sh-UCP2 vector could effectively inhibit the expression of UCP2 in M0 macrophages with an inhibition efficiency of 82.94% (Fig. 4A). UCP2 knockdown was observed to increase the rate of glycolysis and to decrease the level of OXPHOS in M2 macrophages. These effects were significantly attenuated in the presence of the glycolysis inhibitor 2-DG (Fig. 4B and C). In addition, increased glycolysis caused by UCP2 knockdown resulted in increased production of pro-inflammatory cytokines (Fig. 4D-H) and pro-inflammatory chemokines (Fig. 4I-N), but was attenuated by the effect of 2-DG. In addition, sh-UCP2 was observed to contribute to a 66.06% increase in ROS accumulation, but an 18.46% decrease in response to 2-DG (Fig. 4O). These results demonstrated the effect of UCP2 on M1/M2 rebalancing, and thus on reducing inflammation and oxidative stress, is mediated through an effect on macrophage glycolysis.

## Discussion

Metabolic abnormalities are important factors contributing to various diseases, in particular the M1/M2 macrophage imbalance they cause, which is a major obstacle to improving disease outcomes as it can lead to severe inflammatory responses (23). The present study investigated the interplay between macrophage polarization, glycolysis, metabolic reprogramming, ROS and inflammation, focusing on the role of UCP2 in coordinating these processes.

Consistent with previous research (24), the present study observed that M1 macrophages identified by specific markers ($CD86^{+}$) had increased secretion of pro-inflammatory

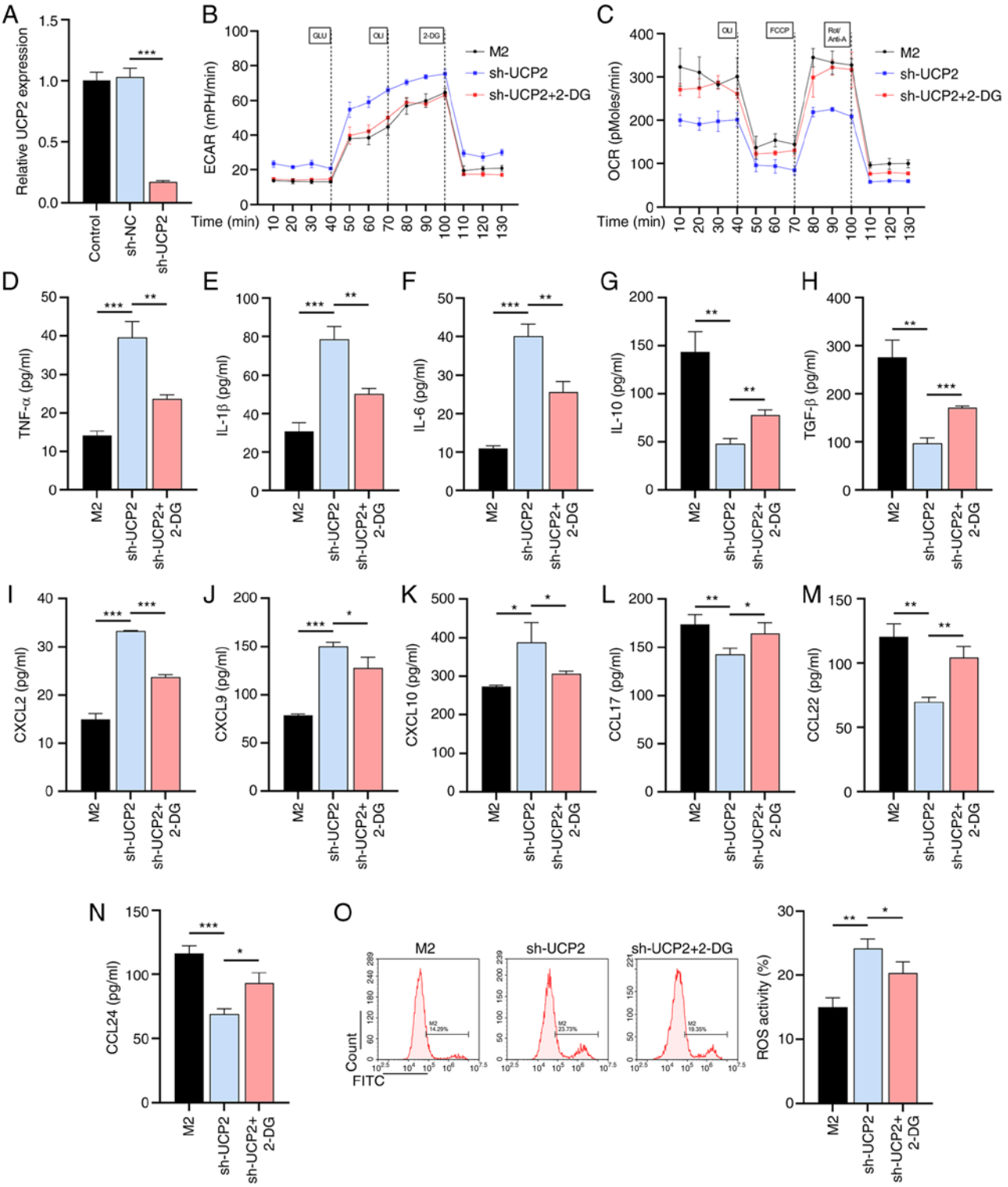


Figure 4. UCP2 knockdown exacerbates inflammation and oxidative stress by promoting macrophage glycolysis. (A) RT-qPCR to verify the validity of the sh-UCP2 vector (n=3). (B) Glycolysis and (C) OXPHOS levels in M2 macrophages with UCP2 knockdown and 2-DG treatment (n=3). ELISA results of pro-inflammatory cytokines (D) TNF-α, (E) IL-1β, (F) IL-6, (G) IL-10 and (H) TGF-β production in UCP2-knockdown M2 macrophages with or without 2-DG treatment (n=3). ELISA results of production of pro-inflammatory chemokines (I) CXCL2, (J) CXCL9, (K) CXCL10, (L) CCL17, (M) CCL22 and (N) CCL24 in UCP2-knockdown M2 macrophages with or without 2-DG treatment (n=3). (O) ROS production in UCP2-knockdown M2 macrophages with or without 2-DG treatment (n=3). $^{*}$P<0.05, $^{**}$P<0.01, $^{***}$P<0.001. 2-DG, 2-deoxy-D-glucose; OXPHOS, oxidative phosphorylation; ROS, reactive oxygen species; IL, interleukin; TNF-α, tumor necrosis factor alpha; CXCL, C-X-C motif chemokine ligand; CCL, C-C motif chemokine ligand; UCP2, uncoupling protein 2; sh-, short hairpin; ECAR, extracellular acidification rate; OCR, $O_2$ consumption rate.

cytokines (TNF-α, IL-1β and IL-6) and decreased UCP2 expression, whereas M2 macrophages ($CD206^{+}$) had increased secretion of anti-inflammatory cytokines (IL-10 and TGF-β) and upregulated UCP2 expression. This suggested that UCP2 may be a key regulator of macrophage phenotypic shifts. As a member of the mitochondrial anion carrier protein family,

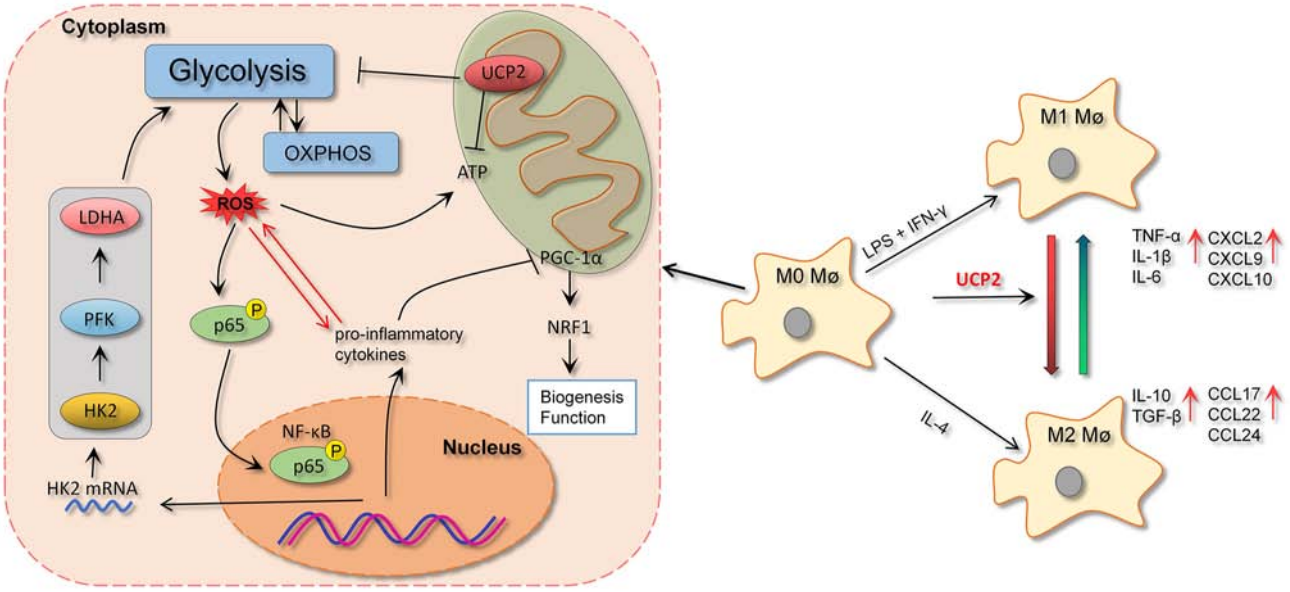


Figure 5. UCP2, by promoting the transformation of M1 macrophages to M2 macrophages, effectively suppresses glycolysis within the macrophages. This action subsequently leads to a reduction in the production of ROS. Furthermore, by minimizing the nuclear translocation of p65, UCP2 also diminishes the secretion of pro-inflammatory cytokines and chemokines, thus serving a pivotal role in modulating inflammation. OXPHOS, oxidative phosphorylation; ROS, reactive oxygen species; IL, interleukin; TNF-α, tumor necrosis factor alpha; CXCL, C-X-C motif chemokine ligand; CCL, C-C motif chemokine ligand; UCP2, uncoupling protein 2; HK2, hexokinase 2; PFK, phosphofructokinase; LDHA, lactate dehydrogenase A; PGC-1α, peroxisome proliferator-activated receptor g coactivator 1-α; NRF1, nuclear respiratory factor 1; P, phosphorylated; LPS, lipopolysaccharide; IFN-γ, interferon γ; Mø, macrophage.

UCP2 is located in the inner mitochondrial membrane and can reduce ROS production by dissipating the proton gradient (25). Under the influence of lentivirus-mediated UCP2 overexpression, all macrophage subtypes exhibited a shift from M1 to M2 polarization, accompanied by reduced ROS production, possibly due to decreased glycolysis (26). The present study confirmed that UCP2 overexpression resulted in decreased glycolysis and key glycolytic enzymes (including HK2, PFK and LDHA) in macrophages with increased OXPHOS. M1 macrophage polarization is induced by LPS and IFN-γ, which are activators of glycolysis (27), suggesting that UCP2 acts as an inhibitor of glycolysis (28). ATP is generated by OXPHOS, the central system of cellular metabolism (29). UCP2 allows protons to leak back across the membrane without passing through ATP synthase, thereby reducing the efficiency of ATP production (30). The present study revealed that UCP2-induced metabolic reprogramming was accompanied by a slight decrease in ATP synthesis and upregulation of mitochondrial biogenesis markers (PGC-1α and NRF1), suggesting that UCP2 may act as a metabolic regulator in macrophages. As reported by Rius-Perez *et al* (31), inflammation-mediated inhibition of PGC-1α may lead to reduced activity of NRF1, a critical factor in maintaining mitochondrial homeostasis.

Notably, the present study showed that UCP2 overexpression resulted in decreased secretion of pro-inflammatory cytokines and chemokines and increased secretion of anti-inflammatory cytokines. This regulation may be achieved through ROS-mediated modulation of signaling pathways involved in cytokine and chemokine expression, such as NF-κB (32,33), and by influencing the metabolic processes controlling their production (34). The current study subsequently confirmed an increase in p65 protein and phosphorylation in M1 macrophages and a decrease in M2 macrophages, with UCP2 promoting reduced p65 protein levels and dephosphorylation in both subtypes.

To further investigate the role of UCP2 in macrophage inflammation and oxidative stress, the present study used a lentivirus-mediated approach to downregulate UCP2 expression in M2 macrophages. Consistent with previous research (35,36), UCP2 downregulation resulted in increased glycolysis rates, decreased OXPHOS levels and increased production of pro-inflammatory cytokines and chemokines, along with increased ROS generation. These results further supported the importance of UCP2 in macrophage function. The observed effects were attenuated by treatment with the glycolysis inhibitor 2-DG, suggesting that the effects of UCP2 on macrophage polarization and inflammation are mediated through the regulation of glycolysis. The findings might have implications for cancer therapy, where tumor-associated macrophages predominantly exhibit an M2 phenotype that supports tumor progression (37). In such circumstances, downregulation of UCP2 might tilt the balance back toward an M1 state, possibly helping to combat tumor growth (38). In general, overexpression of UCP2 reduced glycolysis and increased OXPHOS levels in macrophages. This led to activation of the NF-κB signaling pathway, which ultimately triggered inflammation (Fig. 5). Therefore, understanding the molecular mechanisms underpinning UCP2's regulation of macrophage polarization, could lead to the development of small molecule inhibitors or activators, which may serve as novel therapeutic agents.

The present study had several limitations. First, the mechanisms of UCP2 in specific metabolic diseases were not investigated. Second, numerous non-coding RNAs, such as miRNAs, may play critical regulatory roles in UCP2 expression, which were not investigated in this study. Third, due to the lack of commercially available products that can

directly stimulate glycolysis, this study lacked additional rescue experiments to further confirm the inhibitory effect of UCP2 overexpression on glycolysis in M2 macrophages. Fourth, further *in vivo* studies are needed to further determine the physiological relevance of the present findings, as the complexity of the *in vivo* system may affect macrophage behavior in ways not reflected *in vitro*. Finally, the present study recognized the limitation of not employing single-cell metabolic analyses such as the scMetabolism tool (39). Such an approach could potentially provide additional insights into the metabolic heterogeneity of individual macrophages and further corroborate our findings. Future research could investigate potential pharmacological interventions, such as drugs that enhance or inhibit UCP2 expression or activity. These limitations represent key areas for future investigation and potential therapeutic targets.

In conclusion, the current study demonstrated the important role of UCP2 in regulating macrophage polarization, metabolism, inflammation and oxidative stress through its effects on glycolysis. These findings provide valuable insights into the molecular mechanisms of UCP2 function in macrophages and highlight the potential for developing novel therapeutic strategies targeting UCP2 for macrophage-driven inflammatory and metabolic diseases. By elucidating the importance of UCP2 in macrophage function and its potential implications in immune regulation and inflammation, the present research lays the groundwork for further investigation and potential clinical applications.

**Acknowledgements**

Not applicable.

**Funding**

No funding was received.

**Availability of data and materials**

The datasets used and/or analyzed during the current study are available from the corresponding author on reasonable request.

**Authors' contributions**

LL and DZ designed the experiments. QJ and TM performed the experiments and drafted the manuscript. LL, XM and YY collected and analyzed the data. LL and DZ confirm the authenticity of all the raw data. All authors read and approved the final manuscript.

**Ethics approval and consent to participate**

The study was approved by the Ethics Committee of the People's Hospital of Ningxia Hui Autonomous Region (approval no. 2022316). Written informed consent was obtained from patients.

**Patient consent for publication**

Not applicable.

**Competing interests**

The authors declare that they have no competing interests.

**References**

1. Mahroum N, Alghory A, Kiyak Z, Alwani A, Seida R, Alrais M and Shoenfeld Y: Ferritin-from iron, through inflammation and autoimmunity, to COVID-19. J Autoimmun 126: 102778, 2022.
2. Li C, Xu MM, Wang K, Adler AJ, Vella AT and Zhou B: Macrophage polarization and meta-inflammation. Transl Res 191: 29-44, 2018.
3. Ross EA, Devitt A and Johnson JR: Macrophages: The good, the bad, and the gluttony. Front Immunol 12: 708186, 2021.
4. Viola A, Munari F, Sanchez-Rodriguez R, Scolaro T and Castegna A: The metabolic signature of macrophage responses. Front Immunol 10: 1462, 2019.
5. Zhu L, Zhao Q, Yang T, Ding W and Zhao Y: Cellular metabolism and macrophage functional polarization. Int Rev Immunol 34: 82-100, 2015.
6. Shapouri-Moghaddam A, Mohammadian S, Vazini H, Taghadosi M, Esmaeili SA, Mardani F, Seifi B, Mohammadi A, Afshari JT and Sahebkar A: Macrophage plasticity, polarization, and function in health and disease. J Cell Physiol 233: 6425-6440, 2018.
7. Wang S, Liu G, Li Y and Pan Y: Metabolic reprogramming induces macrophage polarization in the tumor microenvironment. Front Immunol 13: 840029, 2022.
8. Marrocco A and Ortiz LA: Role of metabolic reprogramming in pro-inflammatory cytokine secretion from LPS or silica-activated macrophages. Front Immunol 13: 936167, 2022.
9. Peace CG and O'Neill LA: The role of itaconate in host defense and inflammation. J Clin Invest 132: e148548, 2022.
10. Mouton AJ, Li X, Hall ME and Hall JE: Obesity, hypertension, and cardiac dysfunction: novel roles of immunometabolism in macrophage activation and inflammation. Circ Res 126: 789-806, 2020.
11. van Dierendonck X, Sancerni T, Alves-Guerra MC and Stienstra R: The role of uncoupling protein 2 in macrophages and its impact on obesity-induced adipose tissue inflammation and insulin resistance. J Biol Chem 295: 17535-17548, 2020.
12. Steen KA, Xu H and Bernlohr DA: FABP4/aP2 regulates macrophage redox signaling and inflammasome activation via control of UCP2. Mol Cell Biol 37: e00282-e00216, 2017.
13. Esteves P, Pecqueur C, Ransy C, Esnous C, Lenoir V, Bouillaud F, Bulteau AL, Lombes A, Prip-Buus C, Ricquier D and Alves-Guerra MC: Mitochondrial retrograde signaling mediated by UCP2 inhibits cancer cell proliferation and tumorigenesis. Cancer Res 74: 3971-3982, 2014.
14. Emre Y, Hurtaud C, Karaca M, Nubel T, Zavala F and Ricquier D: Role of uncoupling protein UCP2 in cell-mediated immunity: How macrophage-mediated insulitis is accelerated in a model of autoimmune diabetes. Proc Natl Acad Sci USA 104: 19085-19090, 2007.
15. Nishio K, Qiao S and Yamashita H: Characterization of the differential expression of uncoupling protein 2 and ROS production in differentiated mouse macrophage-cells (Mm1) and the progenitor cells (M1). J Mol Histol 36: 35-44, 2005.
16. Hayden MS and Ghosh S: NF-κB in immunobiology. Cell Res 21: 223-244, 2011.
17. Lawrence T: The nuclear factor NF-kappaB pathway in inflammation. Cold Spring Harb Perspect Biol 1: a001651, 2009.
18. Wang S, Yu H, Gao J, Chen J, He P, Zhong H, Tan X, Staines KA, Macrae VE, Fu X, *et al*: PALMD regulates aortic valve calcification via altered glycolysis and NF-κB-mediated inflammation. J Biol Chem 298: 101887, 2022.
19. Kooshki L, Mahdavi P, Fakhri S, Akkol EK and Khan H: Targeting lactate metabolism and glycolytic pathways in the tumor microenvironment by natural products: A promising strategy in combating cancer. Biofactors 48: 359-383, 2022.
20. Liu H, Zhu S, Han W, Cai Y and Liu C: DMEP induces mitochondrial damage regulated by inhibiting Nrf2 and SIRT1/PGC-1alpha signaling pathways in HepG2 cells. Ecotoxicol Environ Saf 221: 112449, 2021.
21. Zhang Z, Zhang X, Meng L, Gong M, Li J, Shi W, Qiu J, Yang Y, Zhao J, Suo Y, *et al*: Pioglitazone inhibits diabetes-induced atrial mitochondrial oxidative stress and improves mitochondrial biogenesis, dynamics, and function through the PPAR-γ/PGC-1α signaling pathway. Front Pharmacol 12: 658362, 2021.

22. Livak KJ and Schmittgen TD: Analysis of relative gene expression data using real-time quantitative PCR and the 2(-Delta Delta C(T)) method. Methods 25: 402-408, 2001.
23. Kim MJ, Lee H, Chanda D, Thoudam T, Kang HJ, Harris RA and Lee IK: The role of pyruvate metabolism in mitochondrial quality control and inflammation. Mol Cells 46: 259-267, 2023.
24. Tsai CF, Chen GW, Chen YC, Shen CK, Lu DY, Yang LY, Chen JH and Yeh WL: Regulatory effects of quercetin on M1/M2 macrophage polarization and oxidative/antioxidative balance. Nutrients 14: 67, 2021.
25. Forte M, Bianchi F, Cotugno M, Marchitti S, Stanzione R, Maglione V, Sciarretta S, Valenti V, Carnevale R, Versaci F, *et al*: An interplay between UCP2 and ROS protects cells from high-salt-induced injury through autophagy stimulation. Cell Death Dis 12: 919, 2021.
26. Yu J, Shi L, Lin W, Lu B and Zhao Y: UCP2 promotes proliferation and chemoresistance through regulating the NF-κB/β-catenin axis and mitochondrial ROS in gallbladder cancer. Biochem Pharmacol 172: 113745, 2020.
27. Meng L, Lu C, Wu B, Lan C, Mo L, Chen C, Wang X, Zhang N, Lan L, Wang Q, *et al*: Taurine antagonizes macrophages M1 polarization by mitophagy-glycolysis switch blockage via dragging SAM-PP2Ac transmethylation. Front Immunol 12: 648913, 2021.
28. Ji R, Chen W, Wang Y, Gong F, Huang S, Zhong M, Liu Z, Chen Y, Ma L, Yang Z, *et al*: The warburg effect promotes mitochondrial injury regulated by uncoupling protein-2 in septic acute kidney injury. Shock 55: 640-648, 2021.
29. Ahmed ST, Craven L, Russell OM, Turnbull DM and Vincent AE: Diagnosis and treatment of mitochondrial myopathies. Neurotherapeutics 15: 943-953, 2018.
30. Jia JJ, Zhang X, Ge CR and Jois M: The polymorphisms of UCP2 and UCP3 genes associated with fat metabolism, obesity and diabetes. Obes Rev 10: 519-526, 2009.
31. Rius-Perez S, Torres-Cuevas I, Millan I, Ortega AL and Perez S: PGC-1 α, inflammation, and oxidative stress: An integrative view in metabolism. Oxid Med Cell Longev 2020: 1452696, 2020.
32. Morgan MJ and Liu ZG: Crosstalk of reactive oxygen species and NF-κB signaling. Cell Res 21: 103-115, 2011.
33. Korbecki J, Kojder K, Barczak K, Siminska D, Gutowska I, Chlubek D and Baranowska-Bosiacka I: Hypoxia alters the expression of CC chemokines and CC chemokine receptors in a tumor-a literature review. Int J Mol Sci 21: 5647, 2020.
34. Morrissey SM, Zhang F, Ding C, Montoya-Durango DE, Hu X, Yang C, Wang Z, Yuan F, Fox M, Zhang HG, *et al*: Tumor-derived exosomes drive immunosuppressive macrophages in a pre-metastatic niche through glycolytic dominant metabolic reprogramming. Cell Metab 33: 2040-2058 e2010, 2021.
35. Hu S, Feng J, Wang M, Wufuer R, Liu K, Zhang Z and Zhang Y: Nrf1 is an indispensable redox-determining factor for mitochondrial homeostasis by integrating multi-hierarchical regulatory networks. Redox Biol 57: 102470, 2022.
36. Ohkouchi S, Block GJ, Katsha AM, Kanehira M, Ebina M, Kikuchi T, Saijo Y, Nukiwa T and Prockop DJ: Mesenchymal stromal cells protect cancer cells from ROS-induced apoptosis and enhance the Warburg effect by secreting STC1. Mol Ther 20: 417-423, 2012.
37. Li D, Zhang Q, Li L, Chen K, Yang J, Dixit D, Gimple RC, Ci S, Lu C, Hu L, *et al*: beta2-microglobulin maintains glioblastoma stem cells and induces M2-like polarization of tumor-associated macrophages. Cancer Res 82: 3321-3334, 2022.
38. Luby A and Alves-Guerra MC: UCP2 as a cancer target through energy metabolism and oxidative stress control. Int J Mol Sci 23: 15077, 2022.
39. Wu Y, Yang S, Ma J, Chen Z, Song G, Rao D, Cheng Y, Huang S, Liu Y, Jiang S, *et al*: Spatiotemporal immune landscape of colorectal cancer liver metastasis at single-cell level. Cancer Discov 12: 134-153, 2022.